Trajectory Planning for Industrial Robot Manipulators Considering Assigned Velocity and Allowance Under Joint Acceleration Limit

S. Rohan Munasinghe, Masatoshi Nakamura, Satoru Goto, and Nobuhiro Kyura

Abstract: This paper presents an effective trajectory planning algorithm for industrial robot manipulators. Given the end-effector trajectory in Cartesian space, together with the relevant constraints and task specifications, the proposed method is capable of planning the optimum end-effector trajectory. The proposed trajectory planning algorithm considers the joint acceleration limit, end-effector velocity limits, and trajectory allowance. A feedforward compensator is also incorporated in the proposed algorithm to counteract the delay in joint dynamics. The algorithm is carefully designed so that it can be directly adopted with the existing industrial manipulators. The proposed algorithm can be easily programmed for various tasks given the specifications and constraints. A three-dimensional test trajectory was planned with the proposed algorithm and tested with the Performer MK3s industrial manipulator. The results verified effective manipulator performance within the constraints.

Keywords: Industrial robot manipulator, trajectory planning, acceleration constraint, assigned velocity, trajectory allowance.

1. INTRODUCTION

In industrial robotics, trajectory planning is an important part, which determines how well the manipulator performs a given task. Some of the initial work on manipulator trajectory planning can be found in [1], [2], and [3]. Once the end-effector and joint trajectories are planned, any controller can be used to actuate the manipulator to physically realize the planed end-effector performance. Therefore, trajectory planning should consider both controller limits and task specifications so that the expected performance can be realized.

Most industrial robot manipulators today are actuated by PI servo controllers and employed in processes such as welding, cutting, grinding, part handling, etc. There are two major application categories in industrial robotics: (1) positional control and (2) trajectory tracking. In positional control such as part handling, pick and place, etc., the end-effector moves between two pre-specified Cartesian points, and the path it takes in between is not of great importance. In trajectory tracking control such as welding, cutting, painting etc., end-effector Cartesian path and some task specifications are specified a priori. In both categories, joint position trajectories are planned off-line and used to generate control inputs in on-line operation.

Though there is plenty of research on manipulator trajectory planning, the emphasis on the industrial manipulators and existing problems in the industry has not been addressed sufficiently. Nakamura et.al. [4] proposed a planning algorithm for trajectory tracking considering joint acceleration constraint. Munasinghe et. al. [5]. [6] considered assigned end-effector velocity and joint acceleration limit in trajectory planning for positional control and trajectory tracking tasks. Trajectory planning in [7], [8] are objectively similar to this research; however, they are relatively complex to implement in industry.

The specification of trajectory allowance has become an important consideration in industrial robotics today. Allowance is now considered important even in positional control tasks, not only to avoid possible collisions with nearby objects but as a means to exploit the optimum end-effector trajectory. Therefore, it is required that the trajectory allowance be considered in planning the end-effector trajectory. Moreover, trajectory planning for corners while considering optimum velocity should be included in trajectory planning.

Therefore, this research aims at developing an appropriate trajectory planning algorithm for industrial robot manipulators by considering the relevant constraints and specifications. The proposed method plans the end-effector trajectory considering maxi-

Manuscript received June, 14, 2002; accepted: November, 15, 2002.

S. Rohan Munasinghe, Masatoshi Nakamura, and Satoru Goto are with the Department of Advanced Systems Control Engineering, Graduate School of Science and Engineering, Saga University, 1 Honjomachi Saga 840-8502, Japan. (e-mail: rohan @cntl.ee.saga-u.ac.jp).

Nobuhiro Kyura is with the Department of Electrical Engineering, Kinki University, 11-6 Kayanomori, Iizuka 820-8555, Japan.

mum joint acceleration, assigned velocity, and trajectory allowance. Trajectory corners are planned with optimum tangential velocity, whereas a pole-zero cancellation compensator is used for delay dynamics compensation. The proposed trajectory planner was tested with the Performer MK3s industrial manipulator. The results obtained verified the effectiveness of the proposed method.

2. INDUSTRIAL ROBOT MANIPULATOR

2.1. System overview

Fig. 1 illustrates a typical industrial robot manipulator in three degrees of freedom $(\theta_1, \theta_2, \theta_3)$. The reference input generator implements trajectory planning and constructs taught data (u_1, u_2, u_3), which is the time-based joint position trajectories. During operation, it reads joint feedback via an analog to digital converter (ADC) while sending control input via a digital to analog converter (DAC). The servo controller reads control input $w(t)$ and actuates each joint individually. The motion of the joints determines the end-effector motion $P(x,y,z)$ as given by

$$\begin{aligned} x &= [L_1 + L_2 \sin\theta_2 + L_3 \sin(\theta_2 + \theta_3)]\cos\theta_1 \\ y &= [L_1 + L_2 \sin\theta_2 + L_3 \sin(\theta_2 + \theta_3)]\sin\theta_1, \\ z &= L_2 \cos\theta_2 + L_3 \cos(\theta_2 + \theta_3) \end{aligned} \tag{1}$$

Inversely, for a given end-effector position, the corresponding arm configuration can be determined by

$$\begin{aligned} \theta_1 &= \tan^{-1}(y/x) \\ \theta_2 &= \tan^{-1}(c/z) - \cos^{-1}\left(\frac{c^2 + z^2 + L_2^2 - L_3^2}{2L_2\sqrt{c^2 + z^2}}\right), \\ \theta_3 &= \cos^{-1}((c^2 + z^2 - L_2^2 - L_3^2)/(2L_2L_3)) \end{aligned} \tag{2}$$

where L_1, L_2, and L_3 are link lengths of the manipulator and $c = \sqrt{x^2 + y^2} - L_0$. Differentiating (1) the end-effector velocity can be related to joint velocities as

$$\begin{bmatrix} \dot{x} \\ \dot{y} \\ \dot{z} \end{bmatrix} = [\mathbf{J}] \begin{bmatrix} \dot{\theta}_1 \\ \dot{\theta}_2 \\ \dot{\theta}_3 \end{bmatrix} \tag{3}$$

in that Jacobian **J**, is given by

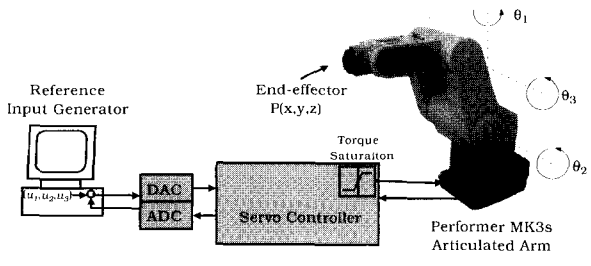

Fig. 1. A typical industrial robot manipulator.

$$\mathbf{J} = \begin{bmatrix} -S_1[L_1 + L_2S_2 + L_3S_{2,3} & C_1[L_2C_2 + L_3C_{23}] & L_3C_1C_{23} \\ C_1[L_1 + L_2S_2 + L_3S_{23}] & S_1[L_2C_2 + L_3C_{23}] & L_3S_1C_{23} \\ 0 & -L_2S_2 - L_3S_{23} & -L_3S_{23} \end{bmatrix}$$

where $S_i = \sin(\theta_i)$, $C_j = \cos(\theta_j)$, $S_{i,j} = \sin(\theta_i + \theta_j)$, and $C_{i,j} = \cos(\theta_i + \theta_j)$.

Joint dynamics of serial link manipulators is highly non-linear, coupled, and used in sophisticated computed torque control schemes as formulated in Lagrange and Newton forms[9] with high computation costs [10]. Due to the inherent complexity, these control schemes are used only in special applications. Industrial robotics, on the other hand, adapt linear gain PI servo control schemes [11], [12] as shown in Fig. 2

The linear manipulator dynamics is assured by limiting values for joint acceleration and velocity. In a typical servo controller as shown in Fig.2, the position loop is P-controlled, whereas the velocity loop is PI-controlled. The operator has to tune the servo parameters K_j^p and K_j^v in order to realize optimum performance. The effects due to varying inertial torques, Coriolis and centripetal torques, and torques due to friction and gravity are considered disturbances, and the linear dynamics can be described by

$$\frac{\Theta_j(s)}{U_j(s)} = \frac{K_j^p K_j^v}{s^2 + 2K_j^v s + K_j^p K_j^v}. \tag{4}$$

2.2. Problem statement

The ultimate objective of robot manipulator control is to achieve desirable end-effector performance. An advanced trajectory planner, which considers

1. Manipulator constraints that assure linear joint dynamics,
2. Specifications that describe desired end-effector performance,

is required to construct appropriate taught data $U(s)$ to assure desirable end-effector performance. Such a trajectory planner should consider the following constraints and specifications:

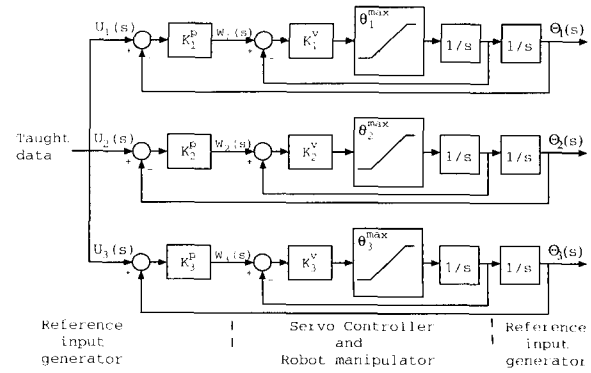

Fig. 2. Second order servo model of manipulator joint dynamics.

$$\left|\ddot{\theta}_j\right| \le \ddot{\theta}_j^{\max} \tag{5}$$

$$v \begin{cases} \le v_a & \text{assigned velocity} \\ \le v_t^{\max} & \text{at corners} \end{cases} \tag{6}$$

$$e \le \rho. \tag{7}$$

Constraint (5) describes maximum joint acceleration, where $\ddot{\theta}_j$ and $\ddot{\theta}_j^{\max}$ stand for joint acceleration and its limit. End-effector velocity specifications are given in (6), where v, v_a, and $v_t^{\max}$ stand for end-effector velocity, assigned velocity, and maximum tangential velocity, respectively. This constraint specifies separate end-effector velocities as it traverses straight lines and circular corners. The trajectory allowance specification is given in (7), where e and ρ represent position error and trajectory allowance in Cartesian space. Any trajectory within the allowance is acceptable, and therefore, the optimum trajectory could be planned. The proposed trajectory planner maintains constraint (5) within the entire operation so that joint dynamics comply with the model given in (4). It also considers the assigned velocity and trajectory allowance and plans the optimum trajectory to achieve desirable end-effector performance.

2.2.1 Determination of joint acceleration limit

The determination process of maximum joint acceleration is usually an iterative experimental procedure in that many criteria could be adapted. Major considerations that govern the maximum joint acceleration are the control input limit and current limit of the servo power amplifier. The joint acceleration limit can be experimentally determined with the violation of any of these two limits. Control input limit violation depends on both trajectory planning criterion and control system design. In addition, it cannot be considered as a valid constraint in trajectory planning. However, the corresponding joint acceleration specifies the limit of linearity, which can be included in constraint (5). Once the joint acceleration limit has been determined, linear dynamics can be guaranteed. This procedure can be applied to most industrial manipulators conveniently to find the respective acceleration limits. Being an experimental procedure, this criterion is model independent.

2.2.2 Determination of assigned end-effector velocity

In manufacturing processes, tasks are resolved into subtasks and performed by individual manipulators. Then, it becomes necessary that the velocity be assigned to each manipulator so that the system of manipulators functions coherently while maintaining the quality of production. The velocity specification, however, is a complicated decision that has to be taken by an expert human supervisor, and the trajectory planner has to plan the realizable trajectory *r(t)*, giving a high priority to maintaining the assigned velocity. Think of a gluing subtask; if the manipulator performs it very slowly, the gluing chemical might set before the pasting subtask starts. On the other hand, if it performs very fast, the quality of the bond will be poor. As such, the expert supervisor has to assign the optimum end-effector velocity in between the two extremes to realize the best performance.

2.2.3 Determination of maximum tangential velocity

The end-effector velocity is significantly lowered as it traverses Cartesian corners in order to avoid acceleration saturation. In the proposed trajectory planning algorithm, a criterion of determining the optimum tangential velocity has been included. This criterion determines $v_t^{\max}$ optimally and drives joint acceleration to its limit without saturation. A complete theoretical derivation of this criterion can be found in [14].

3. TRAJECTORY PLANNING FOR INDUSTRIAL ROBOT MANIPULATORS

3.1. Planning of the realizable trajectory *r(t)*

The proposed trajectory planning algorithm is illustrated in Fig. 3. The objective trajectory *O(s)* is resolved into corners and straight line segments (*a* and *b* in Fig. 3). Trajectories for corners and straight lines are separately planned and merged together. Corners are planned in Cartesian space using constraint (6) and (7) and transformed into joint space using inverse kinematics (2) (*a1* in Fig. 3). Straight line segments are planned in three subsegments, i.e. MJAS (maximum joint acceleration segment), MJDS (maximum joint deceleration segment), and AVS (assigned velocity segment). MJAS and MJDS are planned using constraint (5) provided $v \le v_a$ in (6) is not violated (*b2* in Fig. 3). AVS is planned with assigned end-effector velocity (6) (b3 in Fig.3). Finally, MJAS, AVS, and MJDS are merged and the straight line is planned. Planned corners and straight lines are merged in the respective sequence to obtain the realizable trajectory *R(s)*. The realizable trajectory is compensated by the delay dynamics compensator *F(s)* and taught data *U(s)* is obtained.

3.1.1 Planning of trajectory corners:

Fig. 4(a) shows trajectory planning for a sharp corner *ABC*, considering trajectory allowance ρ. It is proposed to introduce a circular arc in place of a sharp corner, which can be planned within the concentric cylindrical manifold with diameter 2ρ. When a circular arc is introduced replacing a sharp corner as shown in Fig. 5(b), the distance to be travelled is shortened by $DB' + B'E - DHE(arc) = r\{2\cot(\beta/2) - \pi + \beta\}$, where r is the radius of curvature and β is the corner angle.

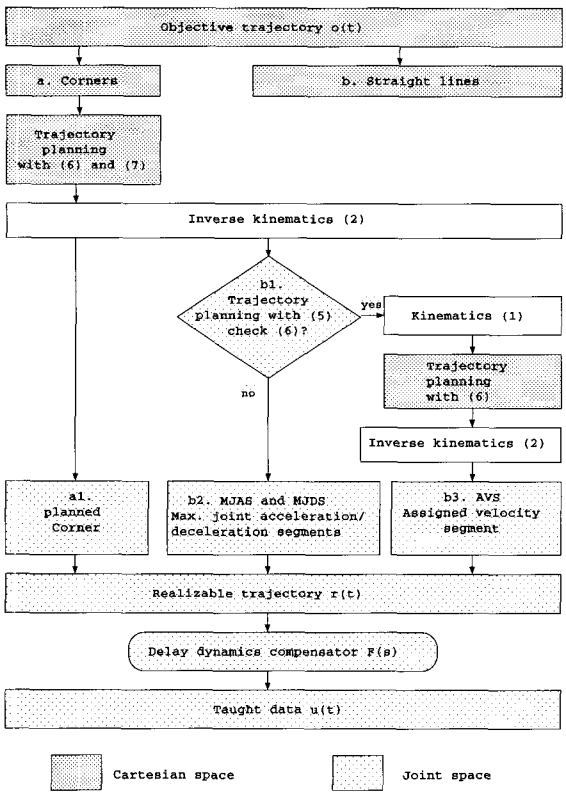

Fig. 3. The proposed trajectory planning algorithm.

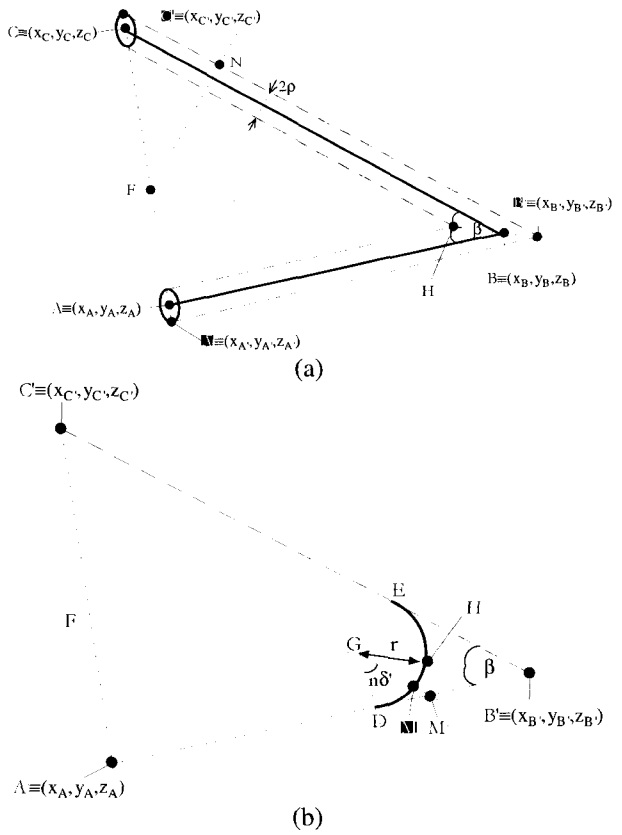

Fig. 4. Trajectory planning for a corner(a). A sharp corner ABC with given allowance, (b). Rounded corner with the largest possible circular trajectory passing through inner point H.

Therefore, increasing r gives a proportional length shortening. Moreover, tangential velocity along the circular arc is $v_t = \sqrt{a_c r}$, where a_c is the centripetal acceleration. Thus, increasing r increases the limit of v_t. As speed reduction is not desirable, it is recommended to increase the radius. In the proposed method, the biggest radius which can be accommodated within the given trajectory allowance is selected, thereby optimizing the two criteria explained above. The optimality criterion for planning the corner refers to the largest radius of curvature within the allowance manifold and the maximum tangential velocity $v_t^{\max}$. Referring to Fig. 4(a), the largest possible circular trajectory should pass through H. Moreover, it should lie on the plane of ΔABC. In order to construct this trajectory, coordinates of A', B', and C' are required, and it can be worked out using co-ordinates of A, B, and C. The planned circular trajectory at the corner is shown in Fig. 4(b) in that radius of curvature r is given by

$$r = 2\rho / \{1 - \sin(\beta/2)\}. \quad (8)$$

With the knowledge of r and all required point co-ordinates, the circular arc can be located accurately. The maximum end-effector velocity $v_t^{\max}$ can be determined so that none of the joints could violate constraint (5) along the circular arc. A detailed treatment of this criterion can be found in [14], and only the criterion equation is given here as

$$v_t^{\max} = \min_j [\max_{\forall j} \{ \sqrt{\ddot{\theta}_j / \phi_j(\theta)} \mid |\ddot{\theta}_j| \le \ddot{\theta}_j^{\max}; \forall \theta \in \xi \}] \quad (9)$$

where ξ is the corner and $\phi_j(\theta)$ is a function of the arm configuration. Using uniform tangential velocity motion, the circular arc is sampled at each $n\delta'$; $n = 1, 2..., N$ as denoted by M in Fig. 4(b), where $\delta' = v_t^{\max} t_s$ is the angle increment corresponding to the sampling interval t_s and $N = (\pi - \beta)/\delta'$.

3.1.2 Planning of straight lines:

Once all corners have been planned, the necessary straight line segments can be identified so that a piece-wise continuous end-effector trajectory can be constructed within the allowance manifold. Fig. 5 illustrates the planning procedure for a straight line segment P_1P_2. Planning of a straight line has three sub-segments to be planned, i.e. MJAS (maximum joint acceleration segment), AVS (assigned velocity segment), and MJDS (maximum joint deceleration segment). The procedure is explained as follows.

P_1P_2 is segmented by a set of equidistant knot points $k=0,1,2....$ Assume at the kth knot, joint j has a velocity $\dot{\theta}_j(k)$ and that it should be moved by $\Delta\theta_j(k) > 0$ to reach the $(k+1)$th knot. It is also necessary to accomplish this motion within the minimum possible

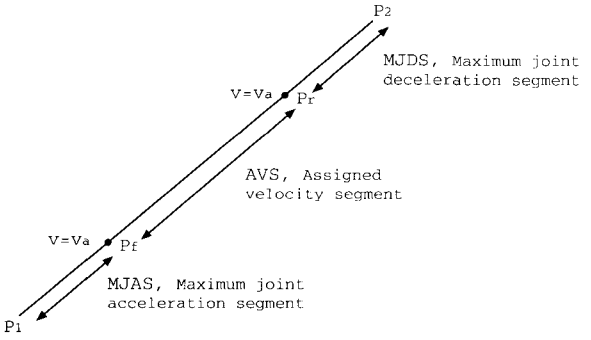

Fig. 5. Trajectory planning for a straight line.

time $t_j^{\min}(k)$. Thus, uniform maximum acceleration motion $\Delta\theta_j(k) = \dot{\theta}_j(k)t_j^{\min} + 0.5\ddot{\theta}_j^{\max}(t_j^{\min})^2$ is used. by rearranging and solving, it gives $t_j^{\min}(k) = \left\{\sqrt{\dot{\theta}_j^2(k) + 2\ddot{\theta}_j^{\max}\Delta\theta_j(k)} - \dot{\theta}_j(k)\right\}/\ddot{\theta}_j^{\max}$. However, if $\Delta\theta_j(k) < 0$, maximum deceleration motion $\Delta\theta_j(k) = \dot{\theta}_j(k)t_j^{\min} - 0.5\ddot{\theta}_j^{\max}(t_j^{\min})^2$ is used, and the corresponding minimum time can be expressed by $t_j^{\min}(k) = \left\{\sqrt{\dot{\theta}_j^2(k) + 2\ddot{\theta}_j^{\max}\Delta\theta_j(k)} + \dot{\theta}_j(k)\right\}/\ddot{\theta}_j^{\max}$. The minimum time duration between the two knot points should be selected as the maximum of $t_j^{\min}; j = 1,2,3,$ so that all joint get at least the minimum time to complete their motions within the acceleration limit. Thus, the minimum inter-knot time duration is given by

$$t^{\min}(k) = \max_j\{t_j^{\max}(k)\}. \tag{10}$$

This time duration is used to determine the uniform joint accelerations of all joints for the motion between the two knot points as given by

$$\ddot{\theta}_j(k) = \frac{2(\Delta\theta_j(k) - \dot{\theta}_j(k)t^{\min}(k))}{\{t^{\min}(k)\}^2}. \tag{11}$$

These uniform joint accelerations are used to plan individual joint trajectories between the two knot points as give by

$$\dot{\theta}_j(k,t) = \dot{\theta}_j(k) + \ddot{\theta}_j(k)t; [kt < t < (k+1)t] \tag{12}$$

$$\theta_j(k,t) = \theta_j(k) + \dot{\theta}_j(k)t + 0.5\ddot{\theta}_j(k); [kt < t < (k+1)t] \tag{13}$$

in that joint velocity $\dot{\theta}_j(k)$ can be determined using the inverse of (3). This algorithm gradually raises the end-effector velocity as it is repeatedly applied with consecutive knot points k=0,1,2...; however, the end-effector velocity should comply with constraint $v \le v_a$ in (6), which is about to be violated at P_F as shown in Fig.5. At this point, MJAS is terminated. The same procedure is used starting from P_2 in the reverse direction in order to plan MJDS, which is terminated at P_r. The remaining part P_fP_r is the AVS, which is planned with $v = v_a$ as given by

$$\begin{bmatrix} x(t) \\ y(t) \\ z(t) \end{bmatrix} = \begin{bmatrix} v_a^x \\ v_a^y \\ v_a^z \end{bmatrix} t + \begin{bmatrix} x(P_f) \\ y(P_f) \\ z(P_f) \end{bmatrix} \tag{14}$$

where v_a^x, v_a^y and v_a^z are the velocity components of v_a along X, Y, and Z axes and $P_f \equiv (x(P_f), y(P_f), z(P_f))$. The AVS is transformed in to joint space using (2) and connected in between MJAS and MJDS so that the entire straight line P_1P_2 is planned.

3.2. Compensation for delay dynamics

The realizable trajectory $R(s)$ is compensated for the delay dynamics as shown in Fig.3. The compensator can be designed based on pole-zero cancellation, as described by

$$F_j(s) = \frac{\mu_1\mu_2(s^2 + K_j^v s + K_j^p K_j v)}{K_j^p K_j^v (s-\mu_1)(s-\mu_2)} \tag{15}$$

where μ_1, μ_2 are the new poles assigned. These poles are tuned by the practitioner in order to realize optimum performance [15]. With the compensator, the system joint dynamics reduces to $F_j(s)G_j(s) = \mu_1\mu_2/\{(s+\mu_1)(s+\mu_2)\}$. Therefore, by tuning these poles μ_1 and μ_2, the delay of joint dynamics can be compensated for.

4. RESULTS AND DISCUSSION

4.1. Simulation and experimental conditions

The objective Cartesian trajectory $o(t)$ was specified by the start point (0.35, 0.00, 0.10)[m], first corner (0.41, 0.10, 0.15)[m], second corner (0.28, -0.10, 0.30)[m], and end point (0.35, 0.00, 0.35)[m]. The trajectory allowance and assigned velocity were set by ρ = 4[mm] and v_a = 0.4[m/s]. Using v_a and ρ, few realizable trajectories were planned with different joint acceleration limits $\ddot{\theta}_j^{\max}$, j = 1,2,3, and the control input $w(t)$ they produce during servoing are observed as in Fig.6.

As expected, higher acceleration limits cause higher control inputs. However, the control input is bounded within ±5[V] (for the Performer MK3 system used in this experiment), which is reached by joint 3 as indicated by ↓A in Fig.6 for the acceleration limit $\ddot{\theta}_j^{\max}$=11.8[rad/s^2], j = 1,2,3. From (8), the calculated radii for the first and second corners were 3.74[mm] and 3.69[mm], respectively. Maximum tangential velocities for the two corners were determined by (9) as 0.205[m/s] and 0.180[m/s]. Velocity loop gain was set by the manufacturer as K_j^v=150[1/s], and position loop gain was tuned to K_j^p=23[1/s], j = 1,2,3. Compensator poles were co-

incidently set by $\mu_1 = \mu_2 = -60$.

Most industrial applications at present adapt the direct sampling technique, the conventional trajectory planning criterion. Simple speed reduction techniques are also practiced without considering optimum settings. To compare with the proposed method, a conventional method was also simulated in that the trajectory was uniformely sampled with the same assigned velocity $v = v_a = 0.4$ [m/s] used in the proposed method.

4.2. Evaluation of results

The end-effector locii, performed by the conventional and proposed methods are illustrated in Fig.7. Huge locus deteriorations occur with the conventional method, whereas the proposed method shows accurate performance with the same assigned velocity. For the proposed method, the end-effector Cartesian position in the XYZ axes are illustrated in Fig.8(a)-(c), and the error of the realized trajectory $y(t)$ is shown in

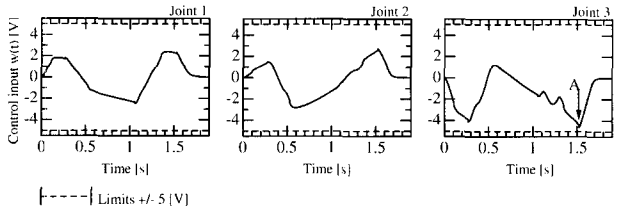

Fig. 6. Control input $w(t)$ of the three joints for $\ddot{\theta}_j^{max} = 11.8$[rad/s^2], j=1,2,3.

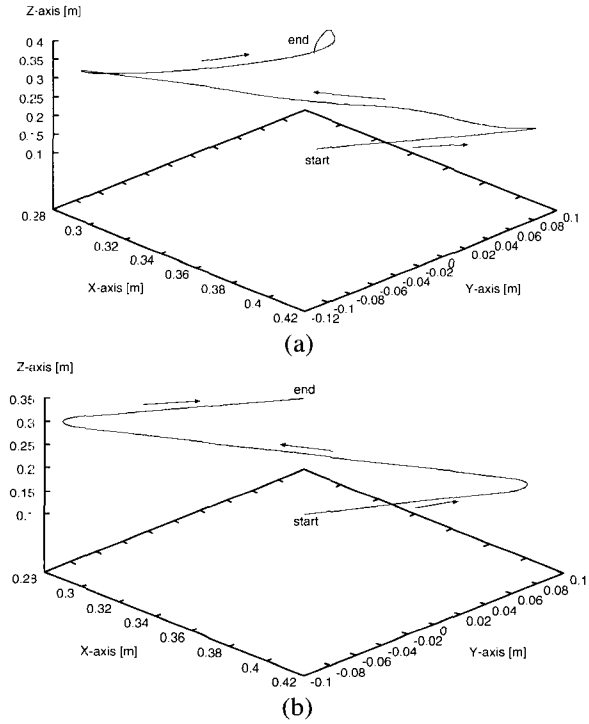

Fig. 7. End-effector locus in Cartesian space (a) conventional method (simulation) and (b) proposed method (experiment) using the same assigned velocity $v_a = 0.4$ [m/s].

Fig.8(d). The realized trajectory $y(t)$ shows a close agreement with the planned realizable trajectory $r(t)$ in all three co-ordinates. The root mean square error remains about 1.7[mm] with the peak 2.9[mm]. Joint accelerations and end-effector velocity results are compared with the conventional method as illustrated in Fig.9. The three columns illustrate simulation results of the conventional method, simulation results of the proposed method, and experimental results of the proposed method, respectively. The first three rows illustrate joint acceleration results, whereas the fourth row illustrates the end-effector velocity. The following evaluations could be drawn by inspection of Fig.9.

1. Simulation and experimental results of the proposed method comply with each other. It indicates the appropriateness of the joint dynamic model and valid selection of constraint limits.

2. The conventional method causes acceleration saturation as partly indicated by C1, C2, and C3 in Fig.9(a),(d), and (g). This behavior could be anticipated without an appropriate trajectory planning at the corners. Acceleration saturation has caused end-effector velocity fluctuations and overshoots as indicated by C4 in Fig.9(j).

3. The proposed method maintains joint acceleration within limits as can be seen in Fig.9(b)-(h). It plans the realizable trajectory $r(t)$ optimally in that at least one joint is actuated with maximum acceleration or deceleration, provided the end-effector velocity complies with (6).

4. At the corners, the proposed method determines maximum end-effector velocities v_t^{max} as indicated by V1 and V2 in Fig.9(k), which drives joint 3 to maximum joint acceleration and deceleration as indicated

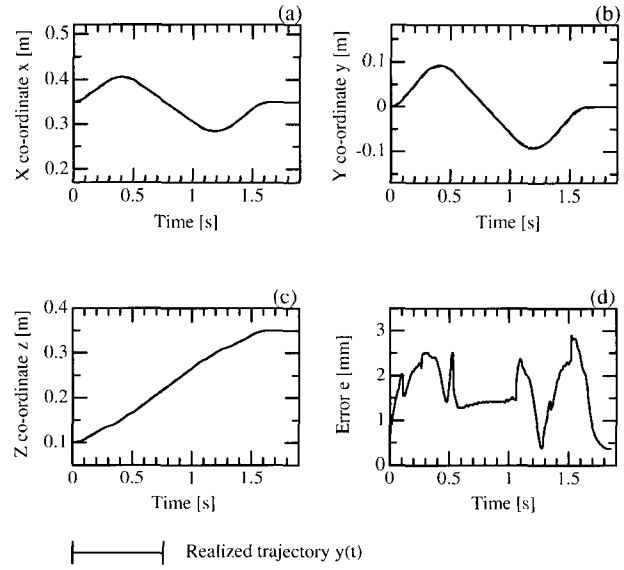

Fig. 8. End-effector performance in Cartesian three-dimension.

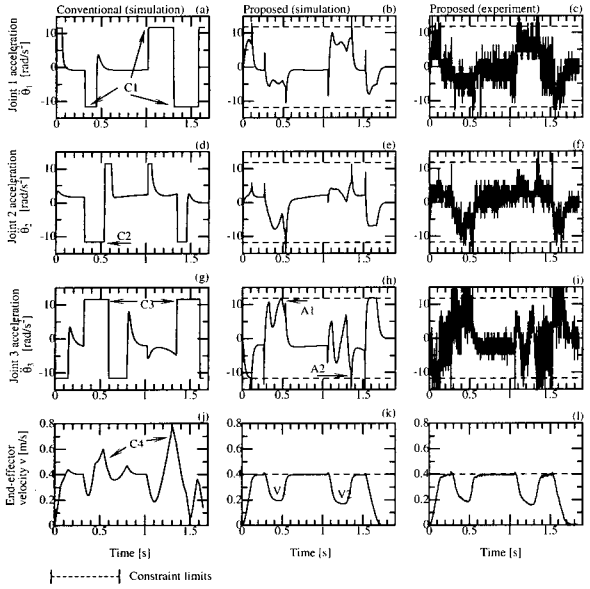

Fig. 9. Results of joint accelerations and end-effector velocity.

of $v_t^{\max}$ by (9) maximizes the end-effector velocity without violating constraint (5).

4.3. Discussion

The realizable trajectory $r(t)$ is planned with separate treatments for corners and straight lines. The most applicable constraints in industrial robotics; e.g.maximum joint acceleration, assigned end-effector velocity, and trajectory allowance are considered in the proposed trajectory planning algorithm. A feedforward compensator is used to compensate the realizable trajectory against the delay in joint dynamics. With all these features, the proposed method is capable of planning the optimum realizable trajectory within the constraints. This research considered only end-effector position trajectory; however, orientation control can also be incorporated in the proposed trajectory planner. As all joints are decoupled and controlled by independent PI servo drives, the first three links can be utilized as the major position control, and the other links can be used for major orientation control. The mutual effects between position and orientation kinematics can be solved and included in the algorithm.

5. CONCLUSIONS

This research presents a new trajectory planning algorithm for industrial robot manipulators, which considers most relevant constraints. The improved performance has been demonstrated and proven by experimentation with an industrial robot manipulator in which a complex three-dimensional end-effector trajectory was performed accurately. The proposed algorithm appears as a feedforward block in the control system. Thus, it can be incorporated with existing industrial manipulators without a significant hardware alteration, cost, or risk. The proposed method can be applied to most industrial applications for effective planning of end-effector trajectories.

REFERENCES

[1] R. H.Taylor, "Planning and execution of straight line manipulator trajectories," *IBM J. Res. Develop.*, vol. 23, no. 4, pp. 424-436, July 1979.

[2] R. Paul, "Manipulator Cartesian path control," *IEEE Trans. on Sys., Man, and Cyber.*, vol. 9, no. 11, pp. 702-711, November 1979.

[3] J. Y. S. Luh and C. S. Lin, "Optimum path planning for mechanical manipulators," *Trans. on the ASME*, vol. 102, pp. 142-151, June 1982.

[4] M. Nakamura, S. R. Munasinghe, S. Goto and N. Kyura, "Enhanced contour control of SCARA robot under torque saturation constraint" *IEEE/ASME Trans. on Mechatronics*, vol. 5, no. 4 pp. 437-440, December 2000.

[5] S. R. Munasinghe, M. Nakamura, S. Goto, S. Aoki and N. Kyura, "High speed precise control of robot arms with assigned speed under torque constraint by trajectory generation in joint coordinates", *IEEE Int. Conf. on Syst., Man, and Cyber.(SMC'99)*, pp. 854-859(II2), October 1999.

[6] S. R. Munasinghe, M. Nakamura, S. Goto, and N. Kyura, "Optimum contouring of industrial robot arms under assigned velocity and torque constraints," *IEEE Trans. on Syst., Man, and Cyber., Part C*, vol. 31, no. 2, pp. 159-167, July 2001.

[7] K. G. Shin, and N. D. Mckay, "Minimum-time control of robotic manipulators with geometric path constraints," *IEEE Trans. on Automat. Cntr.*, vol. 30, no. 6, pp. 531-541, June 1985.

[8] K. G. Shin, and N. D. Mckay, "A dynamic programming approach to trajectory planning of robotic manipulators," *IEEE Trans. on Automat. Cntr.*, vol. 31, no. 6, pp. 491-511, June 1986.

[9] K. S. Fu, R. C. Gonzalez and C. S. G. Lee: *Robotics; Control, Sensing, Vision and Intelligence:*, Singapore: McGraw-Hill, Inc., 1987.

[10] N. A. Aspragathos and J. K. Dimitros, "A comparative study of three methods for robot kinematics," *IEEE Trans. on Syst., Man and Cyber., Part B: Cybernetics*, vol. 28, no. 2, pp. 135-145, April, 1998.

[11] H. G. Sage, M. F. D. Mathelin, and E. Ostertag, "Robust control of robot manipulators: a survey," *Int. Journal of Control*, vol. 72, no. 16, pp. 1498-1522, November 1999.

[12] F. Caccavale, S. Chiaverini and B. Siciliano, "Second-order kinematic control of robot manipulators with Jacobian damped least-squares inverse: Theory and experiments," *IEEE Trans. on Mechatro.*, vol. 2, no. 3, pp. 188-184, Se-

pember 1984.
[13] C. S. Lin, P. R. Chang and J. Y. S. Luh, "Formulation and optimization of cubic polynomial joint trajectories for industrial robots," *IEEE Trans. on Automat. Cntr.*, vol. 28, no. 12, pp. 1066-1074, December 1983.
[14] S. R. Munasinghe, M. Nakamura, "Determination of maximum tangential velocity at trajectory corners in robot manipulator operation under torque constraint," *Proc. Annual Conf. of the Soc. of Inst. and Cntlr. Engineers (SICE)*, CDROM pp. 1170-1175, Osaka, Japan, August 2002.
[15] S. R. Munasinghe, M. Nakamura, S. Goto, and N. Kyura, "Pole selection for modified taught data method for mechatronic servo systems by considering bounded control input," *Proc. Annual Conf. of the Soc. of Inst. and Cntlr. Engineers (SICE), Kyushu Branch*, pp. 183-186, Kagoshima, Japan, December 2001.

S. Rohan Munasinghe received the B.S. and M.S. degrees in Electrical Engineering form the University of Moratuwa, Sri Lanka and Saga University, Japan in 1996 and 1999, respectively. From May 1996 to June 1997 he was with the Department of Electrical Engineering, University of Moratuwa as an Instructor and Lecture. From October 1999 to April 2000, he was with the Department of Computer Science and Engineering, University of Moratuwa Sri Lanka as a Lecturer. Currently, he is pursuing Ph.D. at the Department of Advanced Systems Control Engineering, Saga University, Japan. His research interests include Manipulator Control, Intelligent Control Systems, and Tele/Space robotics.

Masatoshi Nakamura received the B.S., M.S., and Ph.D. degrees in Electrical Engineering from Kyushu University, in 1967, 1969 and 1974, respectively. From 1973 to 1974, he was a Research Associate in Kyushu University. Since 1974, he has been with the Faculty of Science and Engineering, Saga University, where he is currently a Professor in Electrical Engineering. His research interests include Systems Control Theory and its Applications, specially Power System Control, Thermal Flow Control, Robotics and Biomedical Engineering. Prof. Nakamura is a fellow of the Society of Instrument and Control Engineers (SICE) Japan, and a senior member of the IEEE Control Systems Society, the Institute of Electrical Engineers of Japan, the Robotics Society of Japan and the Institute of Systems, Control and Information of Japan.

Satoru Goto received the B.S. and M.S. degrees in Applied Physics from Osaka University, Osaka, Japan, in 1988 and 1990, respectively, and Ph.D degree from Osaka University in 1995. Since 1995, he has been with the Faculty of Science and Engineering, Saga University, Saga, Japan, where he was a Research Associate from 1995 to 1996, a lecturer from 1996 to 1998 and Associate Professor since 1998, in the Department of Advanced Systems Control Engineering. His research interests include Control Theory and its Applications. Dr. Goto is a member of the Society of Instrument and Control Engineers (SICE) Japan, the Robotics Society of Japan and the Institute of Systems, Control and Information of Japan.

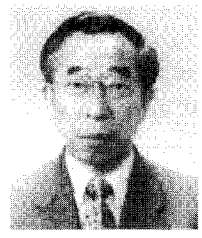

Nobuhiro Kyura received the B.S., M.S., and Ph.D. degrees in Electrical Engineering from Kyushu University in 1964, 1966 and 1992, respectively. Since 1964, he has been with Yasakawa Electric Corporation, Japan, where he is currently the General Manager of the Research Laboratory. Since 1995, he has been with the Department of Electrical Engineering, Kinki University (Kyushu), where he is currently a Professor of Electrical Engineering. His research interests include Motion Controller Architecture, Optimum Motion Control and Robot Manipulator Control. Prof. Kyura received the Outstanding Research Paper Award from the Japan Society of Precision Engineering in 1985. He also received the Outstanding Conference Paper Award "Robot 10", awarded by the Robotics International of SMC (Society of Manufacturing Engineers) in 1986. He is a member of the Institute of Electrical Engineers of Japan, the Society of Instrument and Control Engineers of Japan, the Japan Society of Precision Engineering, the Robotics Society of Japan and the Institute of Systems, Control and Information of Japan.